AIP | Applied Physics Letters

Stable polarization gratings recorded in azo-dye-doped liquid crystals

Suraj P. Gorkhali, Sylvain G. Cloutier, Gregory P. Crawford, and Robert A. Pelcovits

Citation: Appl. Phys. Lett. **88**, 251113 (2006); doi: 10.1063/1.2214176
View online: http://dx.doi.org/10.1063/1.2214176
View Table of Contents: http://apl.aip.org/resource/1/APPLAB/v88/i25
Published by the American Institute of Physics.

Stable polarization gratings recorded in azo-dye-doped liquid crystals

Suraj P. Gorkhali, Sylvain G. Cloutier, and Gregory P. Crawford[a)]
Division of Engineering, Brown University, Providence, Rhode Island 02912

Robert A. Pelcovits
Department of Physics, Brown University, Providence, Rhode Island 02912

(Received 3 January 2006; accepted 7 May 2006; published online 22 June 2006)

We report on the design, fabrication, electro-optical performance, and stability of switchable polarization gratings formed in azo-dye-doped nematic liquid crystals. Stable gratings are demonstrated even after applying saturating electric fields (8 V/μm) and after heating to extreme temperatures (T=190 °C). A simple phenomenological model is presented to show that the Freedericksz threshold voltage depends on surface and volume contributions. The observed thresholdless behavior indicates that the grating stability is consistent with a surface-stabilizing effect. © *2006 American Institute of Physics*. [DOI: 10.1063/1.2214176]

Most conventional holographic gratings are formed using an intensity-modulated interference pattern. In contrast, holographic structures resulting from a polarization-modulated interference pattern are referred to as vectorial or polarization gratings which possess unique diffraction properties.[1–6] However, the most challenging aspects of vectorial holography reside in the difficulty to create permanent structures or to achieve high diffraction efficiencies.[1,7,8] We report on the fabrication and characterization of highly efficient surface-stabilized tunable vectorial holographic gratings recorded in azo-dye-doped liquid crystals (AZOLC) which may enable novel optical devices related to accurate polarization control, measurement, and discrimination.[1,4,7]

Azo-dye molecules can reorient depending on the local polarization of light via photoactivated isomerization.[9] When exposed to light, the excess absorbed energy translates in a conformational change from a *trans*-longitudinal to an unstable *cis*-excited state. The absorbed energy in the *trans* states is proportional to the orientation of the molecular axis with respect to the local polarization due to the anisotropic nature of azo dye. Such an angular dependence will tend to slowly align the dye molecules in the minimal-energy configuration, which is perpendicular to the local polarization. Several reports describe the photoinduced motion of azo dyes in polymers[10] for passive polarization grating applications.[1]

As shown in Fig. 1(a), a one dimensional holographic polarization grating can be formed by the polarization-modulated interference pattern created using two coherent orthogonal circularly polarized beams. The resulting polarization vector modulation in Fig. 1(b) shows a linear polarization which changes orientation periodically along the horizontal axis. Using the basic Jones formalism, Gori has demonstrated that the (±1) first order diffracted beams of such polarization gratings have counter-rotating left and right circular polarizations, respectively, regardless of the incident state of polarization.[7] However, it is also clear from this derivation that the first order diffracted intensities will be strongly dependent on the polarization of the incident beam, resulting in polarization discrimination.[6]

The photoinduced alignment of the azo-dye molecules induces alignment of the liquid crystal molecule.[11] Residori and Petrossian experimentally studied the relative contribution of surface and volume effects in azo-dye-doped liquid crystal.[12] It has also been well established that only a small amount of energy is required to control the bulk orientation of the LC. The alignment induced by the azo dye (as small as 1 mol %) can lead to the orientational alignment of the whole bulk system.[13] The combined photoactivated isomerization of the azo-dye molecules and the strong azo-dye-induced LC alignment is expected to photoalign the LC director perpendicular to the local polarization during the holographic exposure. The photoinduced birefringence of the AZOLC is expected to be much larger due to the contribution of the LC.[12]

A Verdi diode-pumped solid-state laser with an operating wavelength of λ=532 nm was used for the holographic exposure. Orthogonal left and right circularly polarized beams were symmetrically directed to the center of the sample at an incident angle 2α=1.7° which corresponds to a 1.1° angle inside the sample. This small incidence angle reduces the

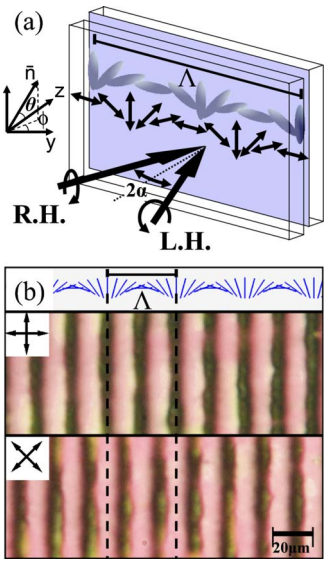

FIG. 1. (Color online) Schematic illustration of the polarization interference pattern and photoinduced alignment distribution of the LC molecules created from the interference of right-handed (RH) and left-handed (LH) circularly polarized light (a). Associated polarization-modulated interference profile (top) and optical microscopy images between crossed polarizers at 0° (middle) and 45° (bottom) (b).

[a)]Electronic mail: gregory_crawford@brown.edu

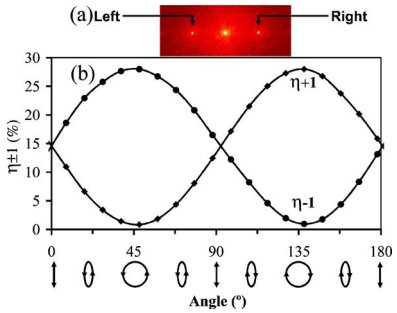

FIG. 2. (Color online) Diffraction pattern using a linearly polarized He–Ne laser (λ=633 nm). Only the first order diffraction spots are observed (a). The diffraction efficiencies in the left η_{-1} and right η_{+1} orders as a function of the ellipticity of the incident probing beam's polarization (b).

overlapping intensity modulation in the interference pattern, which could alter the structure.[1]

The holographic material consisted of a mixture of nematic LC BL038 from EM Industries doped with 4 wt % Disperse Red 1 (DR1) from Aldrich Chemicals. We use BL038 for its large birefringence and excellent properties for optical devices; BL038 has ordinary and extraordinary refractive indices n_o=1.527 and n_e=1.799, respectively, and a dielectric anisotropy $\Delta\varepsilon$=16.4. This AZOLC mixture was sandwiched between indium tin oxide (ITO) coated glass substrates with 20 μm thick spacers. The sample was then exposed to the polarization-modulated interference pattern described above. The incident power density for each beam was 2 W/cm^2 and was exposed four times for 1 min each. The polarization grating created by the interference of the beams is essentially recorded as a periodic spatially modulated LC director orientation inside the sample.

Polarizing microscopy images of the sample oriented at 45° and 90° relative to crossed polarizers are shown in Fig. 1(b). The grating image shifts continuously while rotating the crossed polarizers simultaneously, thus confirming the periodic rotation of the LC molecules. The grating pitch measured 19 μm. Periodically modulating the local alignment of the LC molecules the leads to highly efficient diffraction grating. The sample, when probed with linearly polarized 633 nm He–Ne laser beam at normal incidence, shows strong ±1 first order diffraction spots at the cone angle of 1.9° [Fig. 2(a)]. No significant higher order diffraction was measured, and the +1 and −1 diffracted orders were left and right circularly polarized, respectively, confirming the vectorial grating structure.[7] The diffraction efficiency ($\eta_{\pm 1}$), ratio of the first order intensity to the sum of zero order and higher orders intensities, was measured to be 15% when probed with linearly polarized light.

Figure 2(b) shows the diffraction intensity evolution in ±1 order as a function of the ellipticity of the incident polarization. We used a continuously rotating quarter wave plate to control the ellipticity of the He–Ne probe beam. The evolution shows that the ±1 order intensities are strongly, but oppositely, dependent on the polarization of the incidence beam, indicating a strong polarization-discrimination effect typical of vectorial gratings. The maximum diffraction efficiency ($\eta_{\pm 1}$) is 28% when probed with a circular polarized beam. The linear vectorial anisotropy induced by polarized light can be described using Kakichashvili's elastic model,[8] with $\Delta\varepsilon_{i,j}=\kappa_s S_0 \pm \kappa_v S_1$, where $\Delta\varepsilon$ represents the anisotropic change of a dielectric constant in (i,j) and S_0 and S_1 are the Stokes coefficients representing, respectively, the total intensity of the incoming light $S_0=|E_i|^2+|E_j|^2$ and its preferred polarization orientation $S_1=|E_i|^2-|E_j|^2$.[14] Finally, κ_s and κ_v are the scalar and vectorial photoinduced anisotropy elastic constants, respectively. The diffraction efficiency modulation amplitude shown in Fig. 2 provides a direct measurement of the vectorial photoinduced anisotropy elastic constant κ_v.[1] Experimental results suggest a sevenfold greater vectorial photoinduced anisotropy in AZOLC compared with previous results obtained for the same azo dye alone.[1] Such result should be expected due to the strong molecular anisotropy of the LC molecule combined with the strong orientational ordering of the nematic phase.

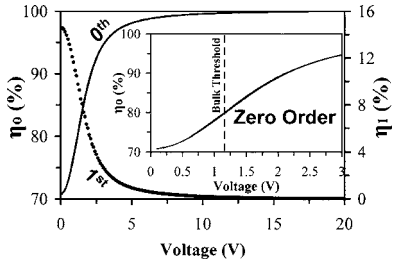

FIG. 3. First order (η_1) and zero order (η_0) diffraction efficiency hysteresis as a function of voltage. There is no quantifiable hysteresis. The inset shows the nature of the zero order threshold.

Under zero-field conditions the LC directors are organized in such a way as to minimize the system's free energy. The LC configuration depends on a delicate interplay between elastic forces, surface boundary conditions, and guest-host molecular interaction. During the exposure, the LC molecules are aligned to form a polarization grating due to interactions between the LC and azo-dye molecules. When a sufficient electric field is applied across the film, LC molecules are homeotropically aligned as a result of the positive dielectric anisotropy of the LC, completely switching off the vectorial grating. The grating completely returns when the voltage is removed. We suspect that the alignment is preserved after exposure due to a residual grating of aligned azo-dye molecules anchored on the substrate surface and acting as an alignment layer.[12] Figure 3 shows the zero order and the first order diffraction intensity evolution as a function of applied voltage. The intensity of the zero order diffraction peak increases as the two first order diffraction peaks disappear with applied voltage. A negligible hysteresis

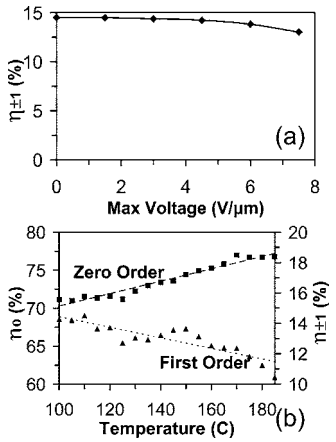

FIG. 4. Diffraction efficiency η_1 measured after application and removal of a high voltage (a), and after the sample was heated above the nematic-isotropic phase transition temperature and allowed to cool at room temperature (b).

exists, and the diffraction efficiency returns to its original value even after multiple switching cycles.

It was previously shown that surface-stabilized liquid crystal gratings should show a pitch-dependent threshold behavior in switching and become threshold less for the case where pitch is comparable to or larger than the cell's thickness ($\Lambda \leqslant d$).[15] However, in AZOLC, volume and surface effects are known to compete with each other.[12] Therefore, the expression for the Frank energy, including the volume energy, can be described as

$$\frac{F}{\Lambda} = K \int_{-\Lambda/2}^{\Lambda/2} dy \int_0^d dz \left\{ \sin^2\theta \left(\frac{d\phi}{dy}\right)^2 + \left(\frac{d\theta}{dz}\right)^2 + 2\sin^2\theta \sin\phi \frac{d\phi}{dy}\frac{d\theta}{dz} - \frac{\Delta\varepsilon\varepsilon_0}{K}(E\cos\theta)^2 - \beta \sin^2\theta \cos^2[\phi - \phi_0(y)] \right\}, \quad (1)$$

where θ and ϕ are the angles between the director and the z and y axes, respectively (see Fig. 1), $\phi_0 = \pi y/\Lambda$ is the angle between the azo-dye molecule and the y axis, d is the cell gap, and Λ is the pitch of the grating. K is the average elastic constant, E is the applied external electric field, $\Delta\varepsilon$ is the dielectric anisotropy of the liquid crystal, and β is a coupling constant between the liquid crystal and azo-dye molecules. Minimizing Eq. (1) yields the following expression for the threshold voltage:

$$V_{\text{th}} = \pi \sqrt{\frac{K}{\Delta\varepsilon\varepsilon_0}} \sqrt{1 - (d/\Lambda)^2 + \beta(d/\pi)^2}. \quad (2)$$

The bulk orienting field of the azo-dye molecules described by the coupling β increases the threshold as the orienting field tends to align the molecules in the x-y plane. Because of this alignment it is energetically less favorable for the material to switch when $\beta \neq 0$. Thus, a higher voltage is required to switch the material in the presence of the bulk orienting field; i.e., the threshold voltage increases with increasing values of β. In the presence of a surface field alone, without the bulk orienting field there is a gain in the Frank elastic energy (going from the nonuniform surface-stabilized state to the switched uniform state). The same gain occurs with the orienting field present but is offset in part by the loss of volume field energy. Assuming $\Lambda = \infty$ and $\beta = 0$ (homogenous alignment), $V_{\text{th}} \cong 1.16$ V using $\Delta\varepsilon = +16.4$ and $K = 2 \times 10^{-11}$ N for BL 038. In our case $\Lambda \sim d$, so the $\Lambda/d \approx 1$. Therefore, the thresholdless electro-optical switching behavior observed in Fig. 3 (inset) constitutes direct supporting evidence for surface-stabilized grating structure, consistent with the previous experimental results reported for such AZOLC systems.[12]

The gratings obtained were stable over the entire period of time required for testing (30 days). To verify their operation stability, we performed rigorous tests under high voltage and high temperature. The samples demonstrated complete switching at 1 V/μm, and this process was carried out for a large number of cycles without any measurable decrease in performance. The diffraction efficiency η_1 evolution measured after a maximum voltage was applied and then removed, as shown in Fig. 4(a). Minimal degradation of the cell was observed even at high saturating electric field strength of 8 V/μm.

To verify the thermal stability and performance, the samples were heated to high temperature and allowed to return to room temperature. When heated above the nematic-isotropic phase transition temperature ($T_{\text{NI}} > 100\ ^\circ$C), the sample transformed into its isotropic state and the grating disappeared as expected. The grating was reproducibly reformed when the temperature was lowered to room temperature, even for temperatures 90 °C above the isotropic transition temperature. The diffraction efficiency η_1 evolution measured at room temperature after the sample was heated over the nematic-isotropic transition point is shown in Fig. 4(b). Even though the polarization grating regained its structure while cooling, its diffraction efficiency decreased only slightly after exposure to high temperatures, as observed in Fig. 4(b). These measurements, along with the thresholdless voltage observation, suggest that the aligned residual molecules near the surface act as an efficient alignment layer to reform the grating following the application of high voltages and after exposure to temperatures above the nematic-isotropic transition temperature.

In summary, we obtained highly efficient and remarkably stable vectorial holographic gratings formed in azo-dye-doped liquid crystals (AZOLC) using the polarization-modulated interference pattern originating from the orthogonal circularly polarized beams. The use of a liquid crystal as a host media for the azo dye allowed for completely reversible electro-optic switching of the vectorial grating structure using an external electric field. The diffraction pattern, polarization microscopy images, and polarization discrimination effects were consistent with theoretical models on polarization gratings. The thresholdless switching behavior and supportive stability measurements are consistent with a surface-stabilized vectorial grating of azo-dye molecules acting as an alignment layer for the liquid crystal.[16] This approach proposes a pathway to achieve electro-optic switching of highly efficient vectorial holographic grating structures with long term stability.

The authors would like to acknowledge NSF Grant No. EEC-0322878 for their financial support. One of the authors (R.A.P.) acknowledge NSF Grant No. DMR-0131573.

[1] S. G. Cloutier, D. A. Peyrot, T. V. Galstian, and R. A. Lessard, J. Opt. A, Pure Appl. Opt. **4**, S228 (2002).
[2] G. Cipparrone, A. Mazzulla, and L. M. Blinov, J. Opt. Soc. Am. B **19**, 1157 (2002).
[3] T. Todorov, L. Nikolova, N. Tomova, and V. Dragostinova, IEEE J. Quantum Electron. **22**, 1262 (1986).
[4] L. Nikolova, T. Todorov, M. Ivanov, F. Andruzzi, S. Hvilsted, and P. Ramanujam, Appl. Opt. **35**, 3835 (1996).
[5] R. Birabassov and T. V. Galstian, J. Opt. Soc. Am. B **18**, 1 (2001).
[6] T. Todorov, L. Nikolova, and N. Tomova, Appl. Opt. **23**, 4588 (1984).
[7] F. Gori, Opt. Lett. **24**, 584 (1999).
[8] S. Kakichashvili, Opt. Spectrosc. **42**, 218 (1977).
[9] Z. Sekkat and M. Dumont, Synth. Met. **54**, 373 (1993).
[10] A. Natansohn and P. Rochon, Chem. Rev. (Washington, D.C.) **102**, 4139 (2002).
[11] S. A. Umanskii, N. V. Novoseletskii, S. I. Torgova, and G. N. Dorozhkina, Mol. Cryst. Liq. Cryst. **412**, 313 (2004).
[12] S. Residori and A. Petrossian, Mol. Cryst. Liq. Cryst. **398**, 137 (2003).
[13] T. Ikeda, J. Mater. Chem. **13**, 2037 (2003).
[14] S. G. Cloutier, J. Phys. D **38**, 3371 (2005).
[15] J. N. Eakin, Y. Xie, R. A. Pelcovits, M. D. Radcliffe, and G. P. Crawford, Appl. Phys. Lett. **85**, 1671 (2004).
[16] S. Residori, G. Russo, S. McConville, and A. Petrosyan, Mol. Cryst. Liq. Cryst. **492**, 111 (2005).